Astron. Astrophys. 221, 236–249 (1989)

ASTRONOMY AND ASTROPHYSICS

The stellar velocity dispersion of the spiral galaxies NGC 6503 and NGC 6340 ⋆

R. Bottema

Kapteyn Astronomical Institute, University of Groningen, P.O. Box 800, NL-9700 AV Groningen, The Netherlands

Received January 13, accepted March 21, 1989

Summary. In this paper the results of long slit spectroscopic observations of the inclined Sc galaxy NGC 6503 and the face-on Sa galaxy NGC 6340 are presented. Modelling of the galactic disk and comparison with the data shows that in NGC 6503 the stellar velocity dispersion in the radial direction is decreasing exponentially with radius, having a scalelength twice the photometric scalelength and central dispersion of 55 ± 10 km s^{-1}. The value of Toomre's Q parameter turns out to be nearly constant throughout the galaxy. Consequently, if a constant Q value is assumed the resulting velocity dispersion values give a good fit to the observed dispersion data. For radii $< 11''$ however, there is a sharp decrease in the velocity dispersion for which a straightforward explanation cannot be given. Numerical calculations suggest that $Q = 1.7$ which implies that the disk of NGC 6503 has a mass-to-light ratio of 1.7 ± 0.3 (in B). This M/L value is in excellent agreement with the result of $M/L_B = 1.7$ obtained from a rotation curve analyses if the so called maximum disk hypothesis applies.

For the nearly face-on Sa galaxy NGC 6340 the perpendicular (or z-direction) velocity dispersion of the disk and the dispersion of the bulge were determined. To this aim a bulge/disk light decomposition was made to be able to determine the influence of bulge and disk on the observed kinematics. For the disk a perpendicular velocity dispersion decreasing exponentially with a scalelength twice the photometric scalelength fits the data very well and at $R = 0$ has the value of 100 ± 20 km s^{-1}. The velocity dispersion of the bulge is around 130 km s^{-1}. Assuming a constant M/L for the disk its value is 4.7 ± 1.5 (in B).

Key words: galaxies – kinematics and dynamics – galaxies: structure – NGC 6340 – NGC 6503

1. Introduction

The study of random stellar motions in galactic disks is not easy, both on the theoretical and observational side. Theoretical work started with the papers by Spitzer and Schwarzschild (1951) and by Toomre (1964) who already showed that knowledge of stellar velocity dispersions is essential for understanding the stability and evolution of galactic disks. Later, numerical work by Ostriker and Peebles (1972), Efstathiou et al al. (1982), Sellwood and Carlberg (1984), and by Athanassoula and Sellwood (1986) learned that cold isolated galactic disks cannot exist. From these studies it also follows that both a massive dark halo and appreciable internal stellar motions in a disk tend to stabilize a galaxy. The papers by Sellwood and Carlberg and by Villumsen (1985) show that a disk heats up, due to the presence of spiral arms, until an equilibrium situation is attained where $Q \sim 1.7$ and the ratio of the vertical to radial velocity dispersion is ~ 0.6, constant with radius. To understand what is actually going on, starting from theoretical basic principles is not possible (Binney and Lacey, 1988) and thus the results of the numerical experiments have to be used to be compared with the observations. This comparison gives useful information about mass content and evolution of galactic disks.

On the observational side progress has been made only in the past few years. For our Galaxy, Lewis (1987) has determined the dispersion for the old disk stars in the radial direction as function of radius. External systems have first been studied by van der Kruit and Freeman (1984, 1986) who showed that the velocity dispersion of the old disk stars decreases with radius in a manner that reconciles constant thickness with a constant M/L ratio. Recent studies by Bottema, van der Kruit and Freeman (1987, hereafter BKF) and by Bottema (1988, called B88) show that both an exponentially decreasing velocity dispersion as function of radius and an approximately constant Q value apply for galactic disks. Also it seems that the more luminous galaxies have a larger velocity dispersion.

In this paper observations are presented and an interpretation is given of the random stellar motions in the inclined Sc galaxy NGC 6503 and the face-on Sa galaxy NGC 6340. In general the results confirm the findings in B88. Section 2 deals with the observations of NGC 6503 and subsequent modelling of the galactic disk in order to determine the radial behaviour of the velocity dispersion. In Sect. 3 this procedure is repeated for NGC 6340 and finally Sect. 4 summarizes the findings and conclusions. Throughout this paper a Hubble constant of 75 km s^{-1} Mpc^{-1} has been adopted.

2. NGC 6503

2.1. A description of the galaxy

NGC 6503 is classified by Sandage and Tammann (1981) as an Sc(s) II.8 galaxy. Photographic three colour photometry in the

⋆ Based on observations obtained with the Isaac Newton Telescope at La Palma which is operated by the RGO at the Observatorio del Roque de los Muchachos of the Instituto Astrofisico de Canarias.

Table 1. Physical parameters of NGC 6503

R.A.(1950)	$17^h\ 49^m\ 58^s$	Shapley-Ames cat.
Declination (1950)	70° 09.5′	"
Hubble type	Sc(s) II.8	"
B_T	10.93	"
Inclination	74°	Begeman (1987)
Pos. angle major axis	121°	"
Max. rotational velocity	120 km/s	"
HI systemic vel.	26 km/s	"
Phot. scale length	40″ for R < 160″ 80″ for R > 160″	Wevers et al. (1986)

U′JF bands has been performed by Wevers et al. (1986) but unfortunately there is only useful information for radii larger than 80″ because the central region is burned out on the plates. A CCD picture of the inner region has been taken (Sect. 2.5) and after combination of the photometry of inner and outer parts it turns out that the photometry of this galaxy can best be described by two scalelengths, $h = 40''$ for $R < 160''$ and $h = 80''$ for $R > 160''$.

The velocity field of NGC 6503 has been mapped using an Hα Fabry-Perot interferometry technique by de Vaucouleurs and Caulet (1982). By averaging over elliptical annuli a rotation curve was constructed for the inner 80″. Neutral hydrogen observations are presented by Shostak et al. (1981), by van Moorsel and Wells (1985) and by Begeman (1987). In the latter two studies a detailed velocity field is presented from which the rotation curve was determined using a least squares fitting procedure. Van Moorsel and Wells find a poor agreement between their HI rotation curve and the Hα rotation by de Vaucouleurs and Caulet in the inner 2′. The difference can be explained by beam smearing affecting the neutral hydrogen observations. The rotation curve by Begeman which has been corrected for beam smearing and the Hα rotation curve are compared with the results presented in this paper. An excellent agreement between the three rotation curves is found. Corrected for galactic rotation the systemic velocity is around 300 km s^{-1}, being so small that it is questionable whether NGC 6503 is taking part in the pure Hubble flow, which would give a distance of 4 Mpc. Based on the Tully-Fisher relation a distance of 5.9 Mpc is found. It is clear that the true distance is debatable, in this paper I shall assume a distance of 6 Mpc. In Table 1 all the relevant parameters for NGC 6503 are summarized and Fig. 1 shows an optical photograph of the galaxy.

2.2. *Observational setup*

The observations were carried out on July 2 and 3 1986, at the observatorio del Roque de los Muchachos on the island of La Palma using the Isaac Newton (2.5 m) telescope. At the Cassegrain focus the intermediate dispersion spectrograph was configured to produce a spectrum with a HPW velocity resolution of ~40 km s^{-1}, centred at a wavelength of 5020 Å. The data were recorded with the Image Photon Counting System (IPCS), having a wavelength range from 4701 to 5394 Å, divided up into 2040 pixels which after converting to a velocity scale resulted in 20.2 km s^{-1} per pixel. The slit which had a length of 4′ covered the South-East or approaching part of the galaxy, along the major axis, together with a sufficient part of the nightsky. This has been indicated on the optical photograph of NGC 6503 (Fig. 1). The spatial extent of the image was distributed over 90 pixels of the detector which results in 90 spectra each with a size of 2″.64 on the sky. During the observations the seeing ranged from 1.0 to 1″.7 and consequently all the spectra along the slit are uncorrelated.

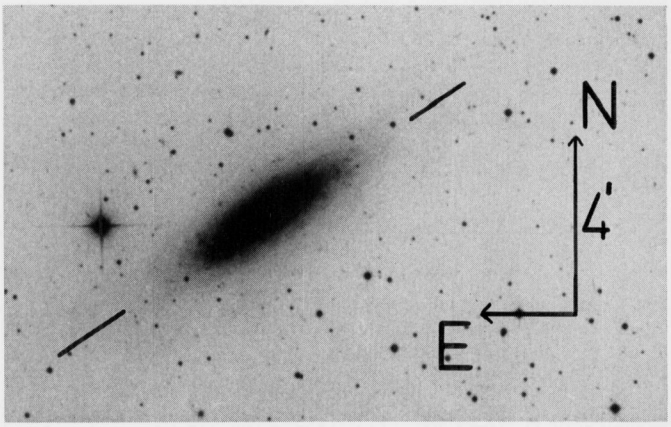

Fig. 1. Optical photograph in the *J*-band of the galaxy NGC 6503. The position of the 4′ long spectrograph slit was (as indicated) along the major axis and covered the South-West part of the galaxy

The total exposure on NGC 6503 lasted for 35400 s ($= 9^h50^m$), divided up into single exposures of ~1200 s. Before and after every exposure the spectrum of a Cu-Ar-Ne lamp was recorded. Also observations of 5 template stars were made, ranging in spectral type from G6III to K2III, which were "sandwiched" between calibration lamp exposures, like the observations of the galaxy. Furthermore the twilight sky, dark current and the image of a "white" lamp were recorded in order to correct the data for any instrumental deviations.

2.3. *Data reduction*

Generally the description of the data reduction is not the most interesting part of a paper. Still, it is a necessary ingredient to enable the reader to assess the quality and precision of the presented data.

For all the 30 2-d spectral images of the galaxy and nightsky the encompassing Cu-Ne-Ar lamp exposures were added. The wavelength calibration was performed by using 26 emission lines evenly spaced over the 693 Å interval. The standard deviation of the lines from the final wavelength solution was never larger than 2 to 3 km s^{-1}. Next the data were regridded to a common log λ scale (20.2 km s^{-1} per pixel) and added to form one calibrated spectral image. For the template star exposures the same procedure was followed. The calibrated stellar spectra were shifted to one common redshift and after this all spectra were averaged to produce one essentially noise free template spectrum.

The white lamp or flat field exposures showed that the pixel-to-pixel variation was less than 2%, which is so small that no corrections were necessary. The dark current of the detector however was quite substantial, about as high as the dark sky. From the total galaxy image the appropriate amount of dark current was subtracted. Next the twilight sky exposures provided the response along the slit for which the data were corrected. A sufficient part at the end of the slit was judged to be essentially free of galaxy light. The spectra in that region were averaged and the result, being the spectrum of the night-sky, was subtracted from the rest of the image. In this way a clean spectral image of the South-East part of NGC 6503 was constructed, ready for further analysis. To get an impression of the countlevels involved, in Fig. 2 the average number of counts over the wavelength range is shown along the slit. The night-sky spectrum has been determined

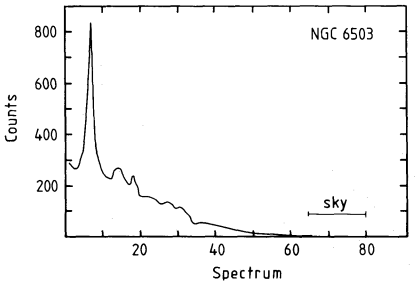

Fig. 2. Average number of counts over the 693 Å spectral wavelength range as function of spectral row along the slit. One spectrum has a size of 2″.64 on the sky

by averaging spectra 65 to 80, while the nucleus is at spectrum no. 7.

2.4. Results of the spectroscopic observations

First the emission line kinematics was determined by measuring the position of the Hβ and O III] 5007 Å lines. Table 2 gives the redshifts, emission line to continuum ratio and Hβ/[O III] flux ratio. The radial velocities as function of distance from the nucleus are plotted in Fig. 3. Because the [O III] 5007 line is weaker the belonging radial velocities show a larger scatter than the Hβ data, but the data points are, considering the errors, in agreement. A proper flux calibration has not been done; the flux ratio of the emission lines is calculated using the assumption that the response of the IPCS is equal for both wavelengths. Judging the efficiency specifications of the IPCS the flux ratio errors will be of the order of 10%. Table 2 shows that near the nucleus the flux of the Hβ line is about half the flux of [O III] 5007 Å. Going to the spiral arm region the ratio rises steeply to about 7 and drops again to ~1 for radii >35″.

The H I systemic velocity of 26 km s^{-1} was used to convert the radial velocities to rotational velocities. These are plotted in Fig. 4 together with the Hα rotation curve determined by de Vaucouleurs and Caulet (1982) and also with the H I rotation curve determined by Begeman (1987). For the inner radii the H I rotation cannot be determined accurately due to beam smearing effects and the Hβ data are based on measurements along the major axis only. Still there is an excellent agreement between the three curves; the differences are comparable or smaller than the errors quoted for the different measurements.

Table 2. Emission line radial velocities of NGC 6503

spectra	distance from max. intensity (arcsec)	Hβ radial vel. (km/s)	Hβ error (km/s)	Hβ emis. int. / cont. int.	[O III] 5007 Å radial vel. (km/s)	[O III] 5007 Å error (km/s)	[O III] 5007 Å emis. int. / cont. int.	Hβ flux / O[III] flux
1	-14.5	74	6	0.85	50	12	0.57	1.5
2	-11.9	63	4	1.2	71	4	0.76	1.6
3	-9.2	55	4	1.02	71	7	0.66	1.5
4	-6.6	57	4	0.78	55	4	0.87	0.9
5	-4.0	51	4	0.80	52	7	1.15	0.7
6	-1.3	54	4	1.22	43	4	1.13	1.1
7	1.3	36	6	1.15	46	4	1.09	1.0
8	4.0	21	4	1.60	14	4	2.64	0.6
9	6.6	24	6	0.54	14	4	1.47	0.4
10	9.2	15	4	0.49	13	8	0.70	0.7
11	11.9	-2	4	0.42	-10	4	0.40	1.1
12	14.5	-24	4	0.53	-8	4	0.66	0.8
13	17.2	-32	5	1.31	-37	4	0.36	3.5
14	19.8	-27	4	0.63	-	-	-	-
15	22.4	-37	4	0.88	-	-	-	-
16	25.1	-41	4	3.67	-51	4	1.19	3.2
17	27.7	-44	5	1.55	-47	4	0.97	1.6
18	30.4	-49	4	4.72	-59	4	1.44	3.2
19	33.0	-48	4	2.00	-44	7	0.50	3.7
20	35.7	-58	4	2.75	-65	10	0.74	3.7
21	38.3	-63	4	5.45	-66	4	1.87	3.0
22	40.9	-60	4	4.39	-68	9	0.75	5.7
23	43.6	-66	4	4.38	-51	6	0.97	4.4
24	46.2	-67	5	2.99	-64	4	0.77	3.5
25	48.8	-60	4	4.24	-68	6	0.83	4.7
26	51.5	-65	4	7.16	-71	4	2.94	2.2
27	54.1	-64	4	6.91	-80	4	2.82	2.4
28	56.8	-61	4	4.92	-71	7	1.44	3.3
29	59.4	-72	5	5.77	-54	9	1.78	3.3
30	62.0	-65	4	6.88	-72	6	1.20	5.2
31	64.7	-62	4	6.49	-76	9	1.26	4.9
32	67.3	-76	4	3.27	-50	5	0.44	6.6
33	70.0	-63	4	2.03	-84	4	0.88	2.4
34:42	83.2	-82	4	0.77	-84	4	0.52	1.4
43	96.4	-82	4	7.95	-87	4	22.6	0.3
44	99.0	-83	4	5.01	-83	4	9.66	0.5
45:47	104.3	-91	6	3.08	-85	4	1.42	1.7
48:60	125.4	-92	6	0.86	-	-	-	-

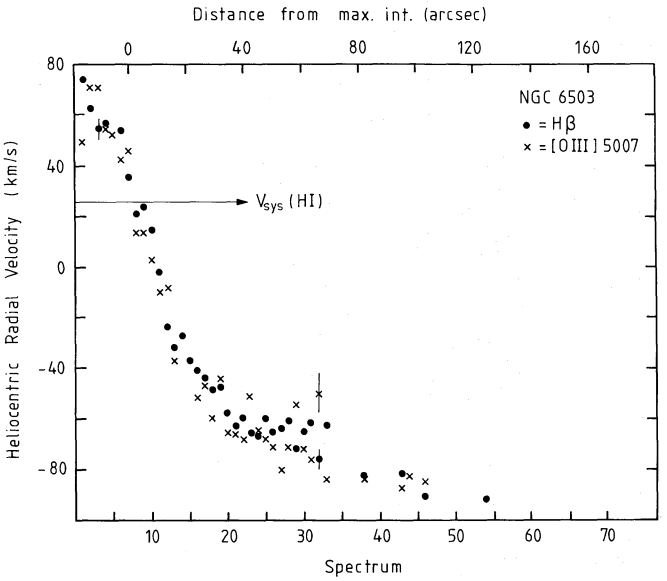

Fig. 3. Emission line radial velocities as a function of position along the major axis. To avoid confusion only for 3 data points the error has been indicated

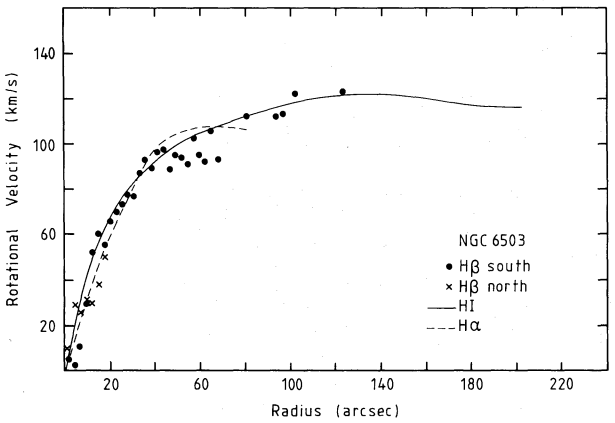

Fig. 4. The Hβ radial velocities converted to rotational velocity. The data have been folded around the H I systemic velocity of 26 km s^{-1}. Comparison with the H I rotation curve derived by Begeman (1987) and with the Hα curve derived by de Vaucouleurs and Caulet (1982) shows an excellent agreement

Some further manipulation of the data is needed to determine the stellar kinematics. The scheme as described in B88 has been followed. The continuum was determined by fitting a polynomial to the spectra and subsequently all spectra were divided by this continuum level. Next the emission lines were removed and then the galaxy spectrum was correlated with the template doing the proper masking, filtering and normalizing. The position of the cross-correlation peak gives the stellar redshift, which was determined by fitting a fourth order polynomial to the peak region. Table 3 gives the stellar radial velocities which are also plotted in Fig. 5 together with a spline function fitted to the Hβ points. An asymmetric drift is not noticeable, as expected because for such a small galaxy the asymmetric drift will be at most a few km s^{-1}.

The stellar velocity dispersions and line strengths are determined by fitting standard cross-correlation functions to the observed peaks. The numerical results are in Table 4. Figure 6 shows all the peaks derived from the observations together with

Table 3. Stellar radial velocities of NGC 6503

spectra	counts	distance from max. intensity (arcsec)	radial velocity (km/s)	error (km/s)
1	~ 200	-14.5	58	4
2	280	-11.9	64	5
3	267	-9.2	59	4
4	301	-6.6	47	4
5	355	-4.0	48	4
6	541	-1.3	40	4
7	835	1.3	28	4
8	376	4.0	12	4
9	303	6.6	13	4
10	245	9.2	10	4
11	226	11.9	-8	5
12	219	14.5	-10	4
13	238	17.2	-22	4
14	268	19.8	-27	4
15	245	22.4	-29	4
16	219	25.1	-35	5
17	199	27.7	-40	4
18	243	30.4	-51	4
19	197	33.0	-56	4
20	151	35.6	-56	4
21	160	38.3	-52	5
22	163	40.9	-63	4
23	154	43.6	-59	4
24	156	46.2	-65	4
25:26	246	50.2	-65	5
27:28	268	55.4	-75	4
29:30	205	60.7	-83	4
31:32	206	66.0	-79	4
33:35	173	72.6	-76	6
36:38	163	80.5	-76	4
39:42	168	89.8	-78	5
41:50	258	103.0	-86	20

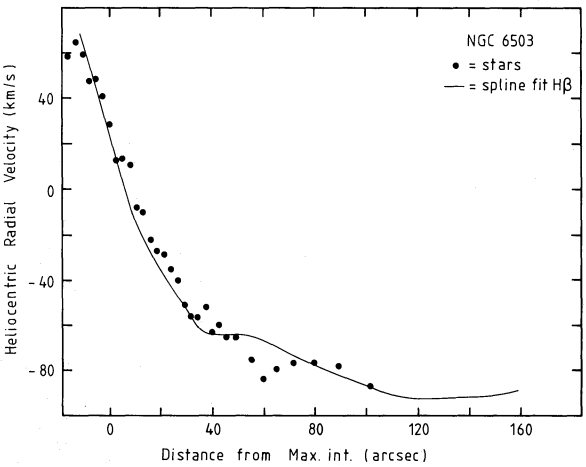

Fig. 5. Stellar radial velocities as a function of radius compared with a spline fit to the Hβ data

the best fitting standard cross-correlation function. Beware of the fact that the line strength parameter given in Table 4 only indicates how good the galaxy spectra resemble the template spectrum. So, a change in stellar population also influences the magnitude of this parameter. The line strength value decreases from 0.5 near the nucleus to ~0.3 at the outer measured radii.

Table 4. Stellar velocity dispersions of NGC 6503

No.	spectra	counts	redshift (km/s)	line strength	dispersion (km/s)	error (km/s)
1	1	~ 200	58	?	47	5
2	2	280	64	0.44	52	10
3	3	267	59	0.47	45	5
4	4	301	47	0.52	45	5
5	5	355	48	0.51	32	5
6	6	541	40	0.52	25	3
7	7	835	28	0.46	25	3
8	8	376	12	0.51	31	3
9	9	303	13	0.52	37	3
10	10:11	471	0	0.49	42	5
11	12:13	457	-15	0.48	44	10
12	14:15	513	-28	0.43	30	7
13	16:17	418	-38	0.45	33	10
14	18:19	440	-53	0.40	29	7
15	20:21	311	-54	0.34	18	7
16	22:23	417	-60	0.36	25	7
17	24:26	402	-66	0.31	23	10
18	27:30	473	-81	0.29	18	7
19	31:34	325	-74	0.22	20	10
20	35:40	310	-69	0.26	17	10
21	41:50	258	-87	0.16	< 30	-

Usually for the correlation between two different template stars this "strength" parameter is between 0.8 and 0.9.

And now the most important result: the stellar velocity dispersions. Figure 7 shows the dispersion as function of distance from the nucleus. For radii larger than 11″ the observed dispersion smoothly decreases from $\sim 45\,\mathrm{km\,s^{-1}}$ to values just below $20\,\mathrm{km\,s^{-1}}$ near a radius around two photometric scalelengths (=80″). There is, however, a sudden drop of the dispersion near the nucleus. This has not been observed for other spiral galaxies. In the following sections a disk model will be employed to determine exactly how the observed values relate to the real internal velocity dispersions as function of radius.

2.5. *Photometry*

For radii larger than 80″ the photometry of NGC 6503 is described by Wevers et al. (1986). Using photographic plates, these authors derived radial profiles in the U', J and F bands. There is a clear bend in the profile around 160″, for smaller radii the scalelength is about 40″ and for the outer parts about 80″. The colour is constant over the extent of the disk, around $B-V=0.8$. Due to overexposure Wevers et al. have no data for the inner parts where almost all spectroscopic measurements are performed.

Thus, not to rely completely on an extrapolation inwards, a CCD picture of the galaxy was needed. Reynier Peletier has been so kind to take two CCD frames, one in the Johnson B and one in the Cousins R band. For this the Jacobus Kapteyn (1 m) telescope on the island of La Palma was used. The detector was an RCA-CCD chip which had a size of 320 × 512 pixels, each pixel a size of 0″.42 × 0″.42 on the sky. The nucleus was put on the centre and the North-South direction along the long side (512) of the chip. NGC 6503 has a position angle of 121° and thus with this setup the major axis runs out of the chip for radii >70″. There were considerable patches on the top and bottoms, which were free of galactic light and could be used to determine the skylevel.

A photograph of the CCD image as it appeared on the tv screen is presented in Fig. 8. As can be seen, the most salient feature is a small bright spot in the centre of the galaxy with a diameter of about 6″, probably to small to call it a bulge. In the inner 30″ there is a lot of small scale spiral structure with a fair number of absorption lanes and patches. For larger radii the galaxy becomes much smoother, with some isolated H II regions, and as can be seen in Fig. 1 the outer parts are very smooth with hardly any spiral structure.

The data reduction proceeded in the standard way. First the bias level was subtracted from all images. Then the flat field images (in B and R) taken on the twilight sky were normalized and the data divided by these. Stars, chip defects and cosmic rays were taken out. The radial luminosity profiles for the B and R image were determined by averaging the intensity along ellipses which were centred on the bright spot and had a fixed ellipticity and position angle given by the photometry of the outer parts. A full ellipse fit (fitting the eccentricity and position angle) to the data has been attempted but did not give a satisfactory answer for $R<40''$ due to the patchiness of the galaxy. To perform the absolute photometric calibration, aperture photometry has been simulated and the results compared with the values given by Longo and de Vaucouleurs (1983).

Table 5 gives the intensity and colour along the major axis; the sky brightness turned out to be $22.39\pm0.08\,\mathrm{mag\,arcsec^{-2}}$ in B and 21.03 ± 0.2 in R. In Fig. 9 the photometric data are shown graphically, together with the values given by Wevers et al. converted to the B and R band. For this conversion relation 1a and 1b were used, derived by Wevers (1984) and relation 1c which is an average relation derived using synthetic colours from the Gunn and Stryker (1983) stellar library:

$$B-V=(J-F)/1.25\,, \tag{1a}$$

$$B=J+0.24\,(B-V)\,, \tag{1b}$$

$$V-R=0.465\,(B-V)+0.098\,. \tag{1c}$$

This results in

$$R=0.018\,J+0.982\,F-0.098\,, \tag{2}$$

showing that the R band is similar to the F band used by Wevers. Comparing the CCD results with the photographic data, the differences are not larger than ~0.15 mag. The most likely explanation for this discrepancy is the fact that for $R>70''$ the major axis part of the galaxy falls out of the CCD chip, only allowing a fit to a part of the disk.

The radial luminosity profile is a typical type II example as defined by Freeman (1970). In the B band the brightness remains almost constant for radii between 15 and 40″. This effect is also present in R but less pronounced, resulting in a $B-R$ colour of 1.4 being ~0.2 mag larger than for the rest of the galaxy. Freeman explains (at least for S0 galaxies) the plateau in the luminosity profile by a real deficiency of light. For NGC 6503 however, most of this effect should be explained by dust because at those radii the galaxy shows the presence of lots of dusty regions which are again responsible for the reddening at that position. A good fit to the data is given by an exponential disk with a scalelength of 40″, which is indicated by the straight line in Fig. 9. This is valid for both colours over a large range of radii implying that there are no large changes in population mix over the extent of the galaxy. The central extrapolated surface brightness is $19.45\pm0.1\,\mathrm{mag\,arcsec^{-2}}$ in B and 18.2 ± 0.1 in R; converted to face-on the values are 20.85 and $19.6\,\mathrm{mag\,arcsec^{-2}}$ respectively. Photographic photometry of the inner region of NGC 6503 exists by Bertola and Bernacca (1967). These observations have been re-analysed by de Vaucouleurs and Caulet (1982) who present the B-band luminosity profile

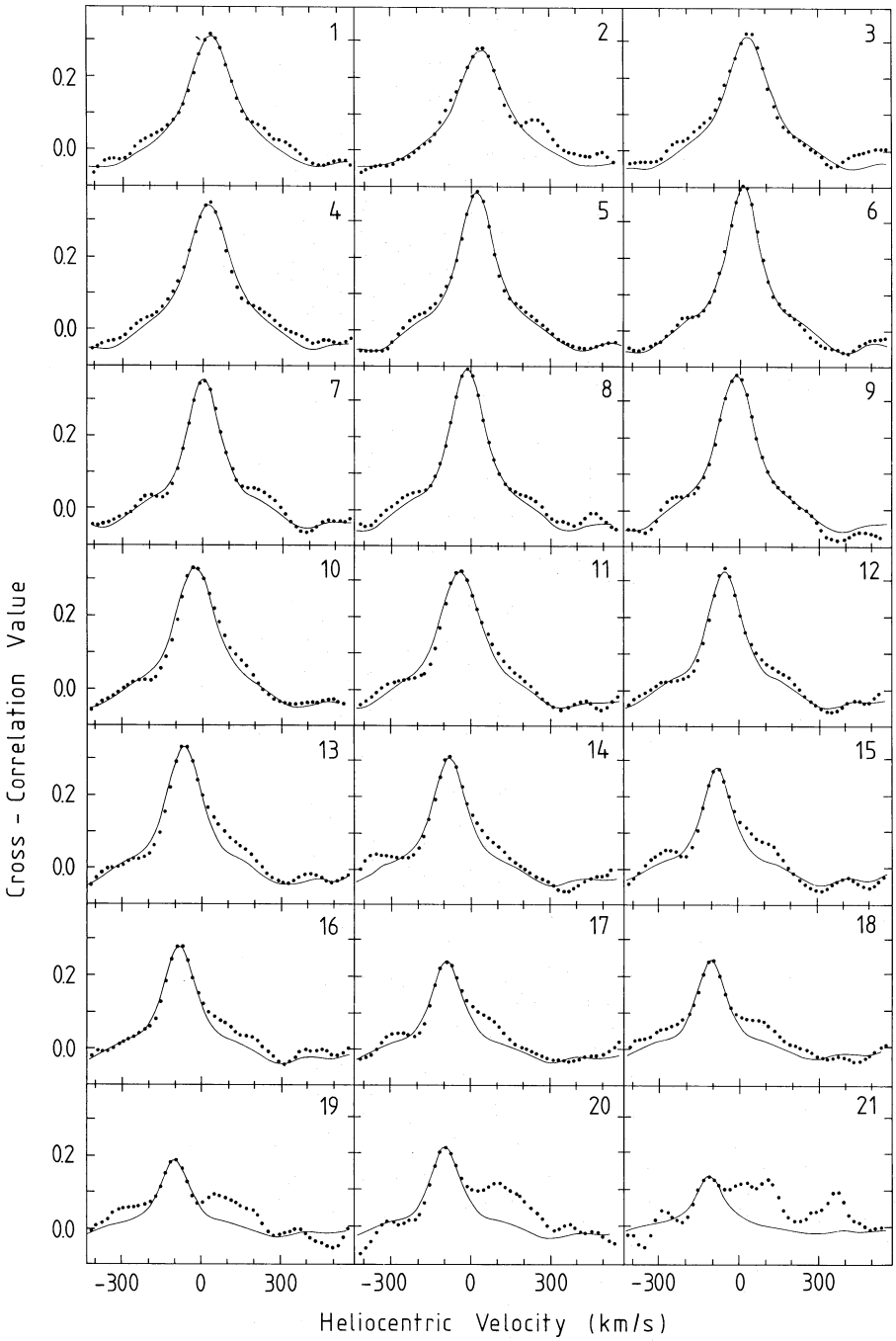

Fig. 6. The observed cross-correlation peaks (dots) with the best fitting model cross-correlation function (line) superposed. The numbers in the top right correspond to the numbers in Table 4

in their Fig. 8. Comparison of the CCD photometry presented here with these earlier observations shows an excellent agreement.

2.6. *The kinematics of the disk*

The observed velocity dispersions have to be related to the real stellar dispersion in the disk. To this aim a disk model will be constructed and its properties compared with the data. In van der Kruit and Freeman (1986) the basic dynamical equations for galactic disks are given and formulas are derived for the asymmetric drift and velocity dispersion as a function of radius. These derivations will not be repeated here, instead a resumé will be given of the most important relations.

For the 3-d density distribution a locally isothermal selfgravitating disk has been assumed:

$$\varrho = \varrho_0 \, e^{-R/h} \, \mathrm{sech}^2\left(\frac{z}{z_0}\right). \tag{3}$$

A constant M/L ratio and thickness z_0 implies that the stellar velocity dispersion in the direction perpendicular to the plane of the disk decreases exponentially with a scalelength twice the photometric scalelength. If the z-direction velocity dispersion is proportional to the radial direction velocity dispersion one might expect that

$$\langle v_R^2 \rangle^{1/2} \propto e^{-R/2h}. \tag{4}$$

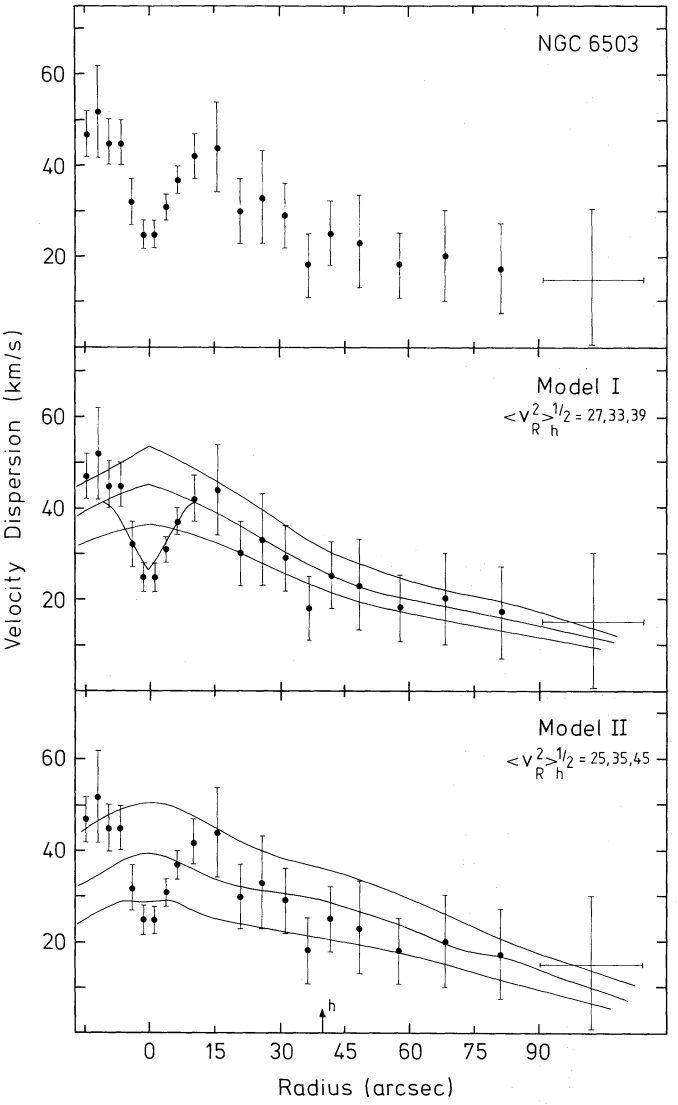

Fig. 7. *Top:* the velocity dispersion data as function of radius. Note the sharp decrease near the centre. *Middle:* the same dispersion data together with the results of the numerical simulation of a model galactic disk with an exponentially decreasing velocity dispersion in the radial direction with a scalelength twice the photometric scalelength ($\langle v_R^2\rangle^{1/2} \propto e^{-R/2h}$). It is concluded that $\langle v_R^2\rangle^{1/2}_{R=h} = 33 \pm 6\,\mathrm{km\,s^{-1}}$. The central depression can only be explained by a drop to almost zero velocity dispersion near the centre (see Fig. 9). *Bottom:* the same as the middle panel but now for an assumed constant Q value as function of radius. These curves also follow the data quite satisfactorily

A disk with such a dispersion behaviour will (as in B88) be called model I.

On the other hand, if one assumes a constant value of Toomre's Q (Toomre, 1964) the radial velocity dispersion varies as

$$\langle v_R^2\rangle^{1/2} \propto \frac{Q}{\kappa}\, e^{-R/h}\, [\sqrt{B(B-A)}]^{-1}, \qquad (5)$$

where κ is the epicyclic frequency and A and B the Oort constants. A constant Q value may be expected if the disk is in equilibrium and the heating process is dependent upon the presence of instabilities like density waves (Carlberg and Sellwood, 1985). This model will from now on be called model II. The results of both disk models will be compared with the observations.

Along the line of sight, going through the galactic disk an integral line profile will develop. This process is simulated; going along the line of sight at every position the density is calculated together with the velocity and velocity dispersion ellipsoid. For the dispersion in the radial direction a radial behaviour as in Eqs. (4) and (5) is assumed and the dispersion in the tangential direction is given by

$$\frac{\langle v_\theta^2\rangle}{\langle v_R^2\rangle} = \frac{B}{B-A}. \qquad (6)$$

For a galaxy with an inclination of 74° the dispersion in the z-direction hardly influences the final results. A simple exponential as in Eq. (4) has been assumed with central dispersion of $25\,\mathrm{km\,s^{-1}}$. The rotational velocity is given by a spline fit to the Hβ data points for the inner region and to the H I data for the outer radii. This rotation is then decreased by the asymmetric drift to give the stellar rotation.

Then, finally, for different radii along the slit or major axis gaussians were fitted to the line profiles. The peak of the gaussian gives the radial velocity, and the dispersion can be compared with the observed velocity dispersions. This whole procedure has been described in more detail in BKF.

2.7. *Fitting the observations*

The velocity dispersion which is observed along the slit is a mix of the dispersions in the radial, tangential and z-direction. For the geometry which applies in the case of NGC 6503, being highly inclined and for which the slit is positioned along the major axis, the tangential dispersion provides the major contribution to the observed value.

In Fig. 7 the model velocity dispersion as function of radius are compared with the observations. Model I ($\langle v_R^2\rangle^{1/2} \propto e^{-R/2h}$) with a central velocity dispersion in the radial direction of $55\,\mathrm{km\,s^{-1}}$ gives a good fit to the data for radii $> 10''$. Judging the error of the individual points one has to conclude that the error for $R = 0$ is about $10\,\mathrm{km\,s^{-1}}$, so $\langle v_R^2\rangle^{1/2}_{R=0} = 55 \pm 10\,\mathrm{km\,s^{-1}}$ and $\langle v_R^2\rangle^{1/2}_{R=h} = 33 \pm 6\,\mathrm{km\,s^{-1}}$. For this case, the real internal velocity dispersion in the radial and tangential direction, as function of radius, are shown in Fig. 10.

In the case of model II the fit is marginally poorer, but it certainly cannot be ruled out. For radii between 10 and 20″ the model dispersions are about $10\,\mathrm{km\,s^{-1}}$ too low. For these small radii however, the constant Q concept is not physically valid any more since the velocity dispersion is of the same order of magnitude as the rotational velocity and consequently the epicyclic approximation cannot hold any more. Still Q can of course always be defined mathematically at these radii. The close correspondence between model I and II implies that if the velocity dispersion decreases exponentially ($\propto e^{-R/2h}$) the value of Q is approximately constant with radius. In the next section this will indeed be demonstrated.

What is striking, and not fitted by either model, is the sharp decrease in velocity dispersion for radii $< 10''$. The only way to produce this decrease is to lower the velocity dispersion very steeply near the inner regions. For the best fitting case, namely model I with $\langle v_R^2\rangle^{1/2}_{R=h} = 33\,\mathrm{km\,s^{-1}}$, the velocity dispersion was made to decrease linearly from the value given by model I at $R = 11''$ to $10\,\mathrm{km\,s^{-1}}$ at $R = 0$. The result after integration is shown in Fig. 7 (middle panel); it gives a good fit to the data. An explanation for this phenomenon is hard to give. It looks like a sort of "eye of the storm" effect, centrally there is almost no rotation and also no differential rotation and because this region is

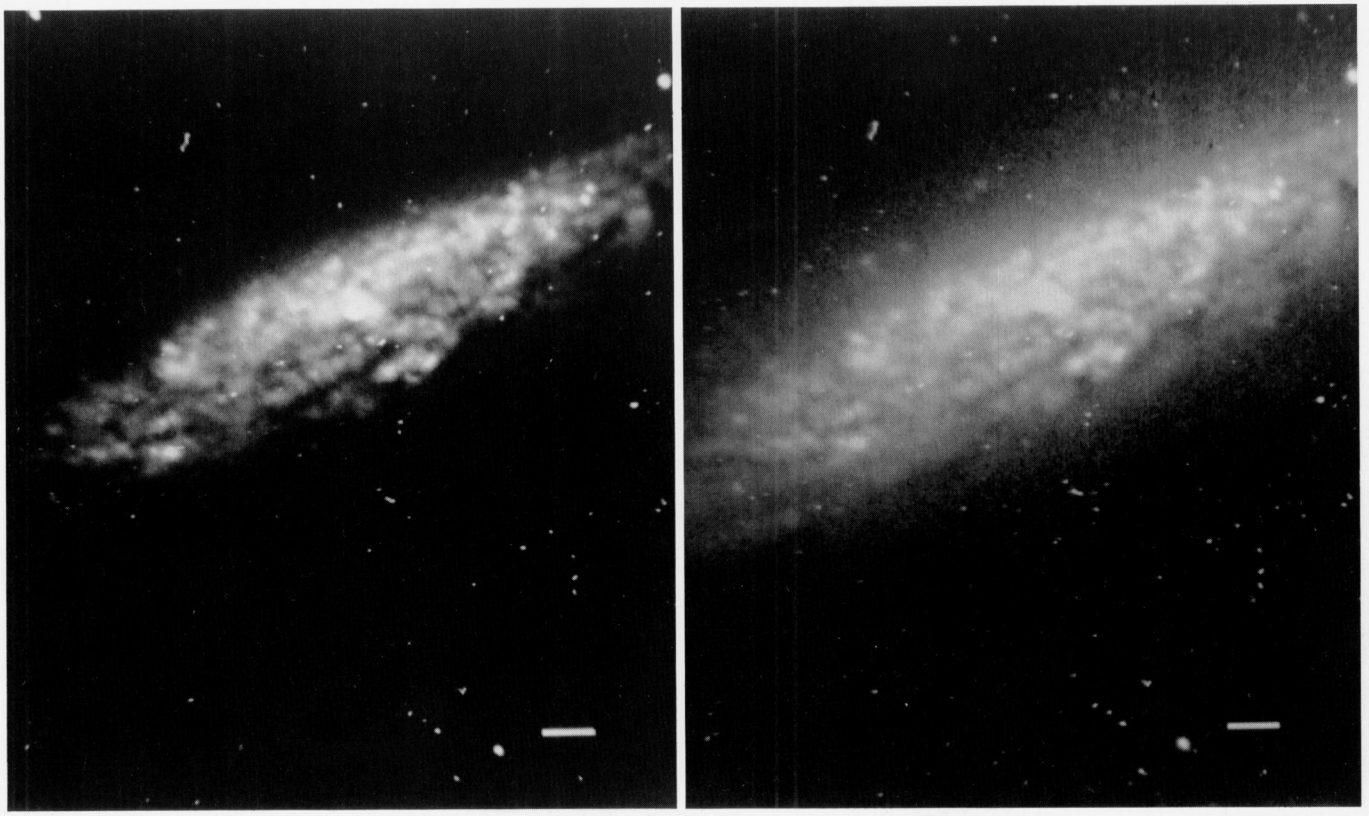

Fig. 8. The CCD image of NGC 6503. *Left:* linear scaling to show the nuclear starlike region. *Right:* the image with a histogram equalization applied to show the spiral arm features. The image has been bias subtracted and flatfielded but the cosmic rays and stars have not been removed. The line in the lower right corner has a length of 10″, North is at top, East on left

so quiet the stars did not acquire a large velocity dispersion at least in the radial direction. The situation becomes more puzzling when one considers the fact that for a locally isothermal stellar disk with constant M/L and thickness the z-direction dispersion has the same radial behaviour as in model I. So if the ratio between z and R dispersion is kept constant throughout the galaxy then the thickness and/or the M/L ratio have to decrease substantially towards the central region.

Some remarks about the asymmetric drift are in order. First, as can be seen from Fig. 5, the stellar rotation is very close to the Hβ rotation. Generally the stars are only rotating a few ($0 \rightarrow \sim 7\,\mathrm{km\,s^{-1}}$) slower than the gas. For the region between 40″ and 70″, where there is a slight plateau in the Hβ rotation, the stars are even going faster which could be caused by a distortion of the gas by a spiral arm. The asymmetric drift calculated for the observed dispersion values amounts to 3–5 $\mathrm{km\,s^{-1}}$, being of the same order of magnitude as the intrinsic velocity errors. Therefore no conclusions concerning the amount of velocity dispersion can be drawn by comparing observed and theoretical asymmetric drift. Integration effects, however, tend to make the stellar radial velocities (as observed) a few $\mathrm{km\,s^{-1}}$ closer to the systemic velocity (BKF). The size of this integration effect depends on the thickness z_0 and by comparing the model with the observations is can be concluded that $z_0 < 0.2\,h$. In other words if the disk is too thick the stars are appearing to rotate too slowly.

2.8. *Stability and mass-to-light ratios*

The velocity dispersions of NGC 6503 which are determined in the previous paragraph are a direct indicator for the disk stability. The best way to describe this is to use Toomre's (1964) criterion which a thin stellar sheet has to obey to be locally stable:

$$Q = \frac{\langle v_R^2 \rangle^{1/2} \kappa}{3.36\, G\sigma} > 1\,, \tag{7}$$

where κ is the epicyclic frequency, $\kappa = 2\sqrt{B(B-A)}$ and σ the projected surface density. As in B88 Q will be treated here as an observable quantity which is compared with results from numerical experiments. As to the validity of this I refer to the paper just mentioned.

For a galactic disk with the properties of NGC 6503 there is little difference in the eventual dispersions between model I (exp. decreasing) and model II (constant Q). First I shall calculate how much deviation from constant Q indeed occurs in the case of model I. To determine Q three parameters are needed: the stellar velocity dispersion, the epicyclic frequency κ and the surface density of the disk. The first parameter is the familiar exponential relation (Eq. 4) with a central R-dispersion of 55 $\mathrm{km\,s^{-1}}$; the epicyclic frequency follows from the rotation curve. To determine the (face-on) surface density (σ) one needs

$$\sigma = L(R) \cdot \left(\frac{M}{L}\right), \tag{8}$$

where $L(R)$ is the face-on surface brightness, here given by $L(R) = L_0\, \mathrm{e}^{-R/h}$. The mass-to-light ratio (M/L) is assumed to be constant throughout the disk. The central surface brightness (L_0) is determined in Sect. 2.5 and amounts to 20.85 mag $\mathrm{arcsec^{-2}}$ in the B band. Conversion gives $L_0^B = 302\, L_\odot\, \mathrm{pc^{-2}}$ and, since a $B-V$ of 0.8 implies that 76% of the light in B originates from the old

Table 5. *B* and *R* band photometry of NGC 6503

radius along major axis (arcsec)	B-band surface brightness (magn. arcsec^{-2})	R-band surface brightness (magn. arcsec^{-2})	B-R colour
1.26	19.24	18.00	1.24
1.52	19.35	18.08	1.27
1.84	19.46	18.17	1.29
2.23	19.57	18.27	1.30
2.70	19.69	18.36	1.33
3.27	19.79	18.45	1.34
3.96	19.88	18.54	1.34
4.78	19.97	18.63	1.36
5.26	20.01	18.68	1.33
5.79	20.07	18.72	1.35
6.37	20.15	18.77	1.38
7.01	20.21	18.82	1.39
7.71	20.25	18.86	1.39
8.48	20.28	18.88	1.40
9.32	20.32	18.91	1.41
10.26	20.35	18.95	1.40
11.28	20.38	18.97	1.41
12.41	20.39	19.00	1.39
13.65	20.41	19.03	1.38
15.02	20.44	19.06	1.38
16.52	20.45	19.08	1.37
18.2	20.45	19.10	1.35
20.0	20.43	19.13	1.30
22.0	20.48	19.17	1.31
24.2	20.50	19.20	1.30
26.6	20.46	19.22	1.24
29.3	20.46	19.24	1.22
32.2	20.51	19.29 ± 0.03	1.22
35.4	20.51	19.33	1.18
39.0	20.55	19.38	1.17
42.8	20.60	19.45	1.15
47.1	20.68	19.55	1.13
51.8	20.85	19.68 ± 0.04	1.17
57.0	20.91	19.81	1.10
62.7	21.13	19.99	1.14
69.0	21.42	20.21	1.21
75.9	21.68 ± 0.04	20.42	1.26
83.5	21.98	20.63 ± 0.10	1.25
91.8	22.17	20.80 ± 0.12	-
101.0	22.41 ± 0.06	21.00 ± 0.13	-
111.1	22.80 ± 0.09	21.23 ± 0.16	-
122.2	23.19 ± 0.12	21.47 ± 0.20	-
134.5	23.71 ± 0.20	21.71 ± 0.25	-
147.9	24.30 ± 0.5		

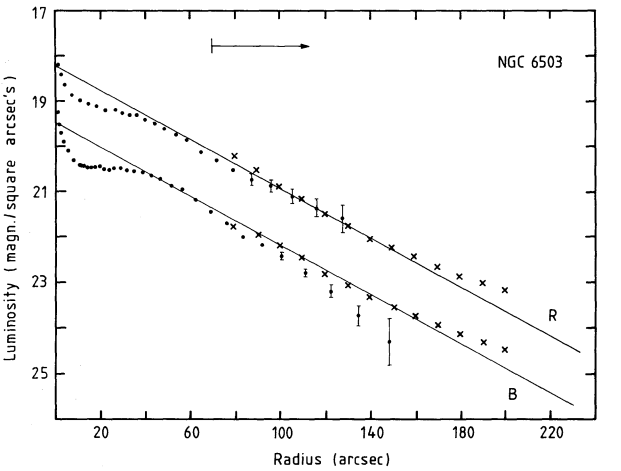

Fig. 9. Surface photometry of NGC 6503 in the Johnson *B* and Cousins *R* bands. The dots represent the CCD data and the crosses the photographic data by Wevers et al (1986) converted to *B* and *R*. The arrow indicates the regions where part of the image fell off the CCD chip. The straight lines represent an exponential disk with a scalelength of 40″

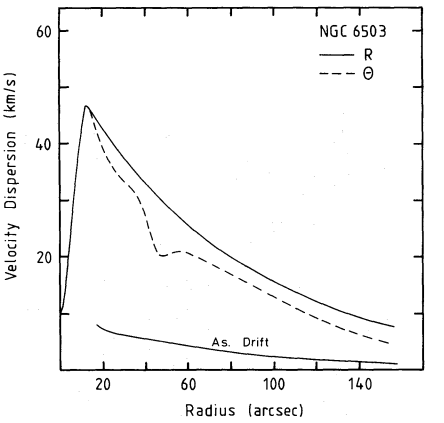

Fig. 10. The real physical velocity dispersion in the *R* and Θ directions used for the best fitting curve in the case of Model I ($\langle v_R^2 \rangle^{1/2} \propto e^{-R/2h}$). Also the small amount of asymmetric drift has been indicated

disk population alone (see B88), this means $L^B_{0,\text{old disk}} = 230 \pm 25\, L_\odot\, \text{pc}^{-2}$. Substituting all the relations into Eq. (7) we get

$$Q = 0.01654 \cdot e^{R/2h} \left(\frac{\kappa}{\text{km s}^{-1}\,\text{kpc}^{-1}}\right) \left(\frac{M/L}{\text{solar units}}\right)^{-1}. \quad (9)$$

For different values of M/L a dependence of Q upon radius is given in Fig. 11. It can be seen that Q is approximately constant.

Numerical experiments using realistic galaxy models and rotation curves (Sellwood and Carlberg, 1984) indicate that indeed the value of Q is constant throughout the disk. For the more realistic models including cooling a Q value around 1.7 is attained for a disk in equilibrium. If this value is used in Fig. 11 the best fitting curve is for a mass-to-light ratio of 2.1 in *B* for the old disk only, taking the errors into account: $(M/L)_{B,\text{old disk}} = 2.1 \pm 0.3$. In the case of model II the values can be substituted directly into Eq. (7) giving also $(M/L)_{B,\text{old disk}} = 2.1 \pm 0.3$ for $Q = 1.7$.

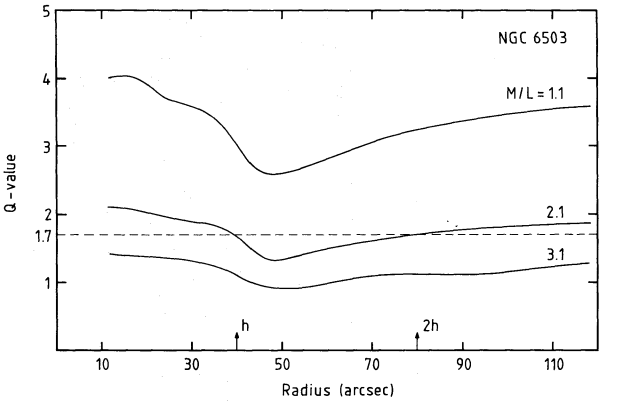

Fig. 11. The change of Toomre's Q value as function of radius for three different M/L ratios (in *B*, old disk only) in the case of Model I. The results of numerical experiments give $Q = 1.7$ which implies $M/L = 2.1 \pm 0.3$ in solar units

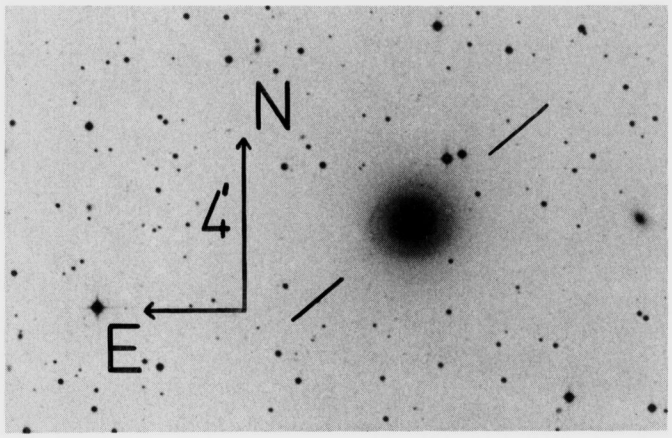

Fig. 12. An optical photograph in the *J* band of the galaxy NGC 6340. The orientation of the slit (4′ long, position angle 130°) has been indicated

For the total, young and old disk population together this gives $(M/L)_B = 1.7 \pm 0.3$. A comparison can be made with the M/L ratio's found by Begeman (1987). He finds a value for the stellar disk of $(M/L)_B < 2.0$ in the case of a fit of the disk photometry alone to the rotation curve. When a dark halo is included in order to fit the rotation curve in the outer regions of the galaxy the disk mass has to be decreased a little and consequently $(M/L)_B < 1.7\, M_\odot/L_\odot$. The smaller than sign can be replaced by an equal sign if the so called maximum disk hypothesis applies. One can see that the M/L value calculated in this paper on the bases of stellar velocity dispersion measurements and the results of numerical calculations is in excellent agreement with Begeman's data, and strongly suggest that the maximum disk hypothesis indeed applies for at least this galaxy. In B88 the also almost pure disk galaxy NGC 3198 was studied and a likewise comparison between M/L ratios was made. For that galaxy the value found from the velocity dispersion was also in good agreement with the maximum disk value.

3. NGC 6340

3.1. *Description of the galaxy*

NGC 6340 is a very regular face-on Sa galaxy with a prominent bulge and a little spiral structure in the disk. Figure 12 shows a photograph in the *J* band with the slit position of the spectrograph indicated. Photometry exists by Wevers et al. (1986) which shows that the radial disk light distribution is very close to exponential with a scalelength of 28″. Taking into account the photometry of the inner 70″ the scalelength for these radii is a little smaller: 25″, which is confirmed by an exponential fit to the light intensity along the spectrograph slit, shown in Fig. 16. For this galaxy there is hardly any radial colour gradient, $B-V \sim 0.92$ for the whole disk.

Three observation periods of 12 h with the Westerbork Synthesis Radio Telescope have been spent to search for H I associated with NGC 6340, two times near a radial velocity of 1900 km s^{-1} and once near 1250 km s^{-1} (Wevers et al., 1986). All these observations gave negative results which is obvious for two of the three observations because, as will be shown in Sect. 3.2, the systemic velocity of this galaxy amounts to 1236 ± 5 km s^{-1}. Hence the radio observations around 1900 km s^{-1} missed the galaxy completely. In this study a distance of 20 Mpc was assumed

Table 6. Physical parameters of NGC 6340

R.A. (1950)	$17^h\ 11^m\ 16^s$	Shapley-Ames cat.
Declination (1950)	72° 21.9′	"
Hubble type	Sa(r) I	"
B_T	11.90	"
Phot. scale length	28″	Wevers et al. (1986)
B-V colour	0.92 magn.	"
Inclination	~ 20°	this study
Systemic velocity	1236 ± 5 km/s	"

which gives a radial scalelength for the disk of 2.4 kpc. Note that the linear dimensions in Wevers et al. are all wrong due to an incorrectly assumed radial velocity, however the numbers quoted by Sandage and Tammann (1981) are correct (they give $V_{sys} = 1234$ km s^{-1}). In Table 6 all the relevant physical parameters of NGC 6340 are summarized.

3.2. *Spectroscopy, setup and results*

NGC 6340 was observed on July 4th, 1986 at the same observatory and with the same instrumentation as for NGC 6503. A different grating was used however, giving a slightly smaller resolution of ~60 km s^{-1}; the spectrum was centred at 5150 Å. The spectrograph slit was turned in a position angle of 130° and its centre was put on the centre of the galaxy. In this way at both ends of the slit the night-sky was observed simultaneously. The total exposure on NGC 6340 lasted for 15150 s ($=4^h12^m$) divided up into single exposures of 1200 s. All exposures were "sandwiched" between calibration images of a Cu-Ar lamp. Also four template stars were observed with type around K0III and images were taken of the twilight sky and dark current.

The spectrum was recorded from 4694 to 5754 Å, divided up into 2040 pixels. For the wavelength calibration 30 lines were used of which the standard deviation from the final wavelength solution was always less than 6 km s^{-1}. All the galaxy images (size 2040×90) were regridded to a common $\log \lambda$ scale with a velocity per pixel of 29.83 km s^{-1} and subsequently the images were added. Corrections for instrumental deviations and the treatment of the template spectra proceeded in the same manner as for NGC 6503. Of the total galaxy image a number of spectra at both ends of the slit were averaged, producing a night-sky spectrum which was subtracted from the rest of the image. Then at the fainter parts spectra were added up to a contlevel of ~200. The spectra at different radii were cross correlated with the template and redshift and velocity dispersion were determined as described in Sect. 2.2 and in B88.

And now the results. Table 7 gives the kinematic values together with radius and countlevels, all the individual cc peaks are shown in Fig. 13 while Figs. 14 and 15 show the radial velocities and velocity dispersions as function of radius respectively. As usual for spiral galaxies, the velocity dispersion decreases going outwards from the centre. At $R = 0$ the value is ~140 km s^{-1} and at one scalelength ~60 km s^{-1}. Although the galaxy is very close to face-on there is still a considerable radial velocity gradient, about 140 km s^{-1} from side to side. The position angle of the slit was chosen at random and the absence of a velocity gradient would have meant that it was positioned along the minor axis. For a galaxy with the luminosity of NGC 6340 one expects a maximum rotation of about 200 km s^{-1} and an inclination of 20° then gives a maximum velocity difference of 140 km s^{-1} along the major axis. Judging the isophotes of NGC 6340 an inclination larger than 20° seems very unlikely and consequently the position

Table 7. Redshift and velocity dispersions of NGC 6340

No.	spectra	counts	radius (arcsec)	redshift (km/s)	error (km/s)	vel. dispersion (km/s)	error (km/s)	bulge/disk ratio
1	20:33	205	-49.37	1160	38	-	-	0
2	34:37	160	-25.61	1178	6	49	5	0
3	38:40	217	-16.37	1177	20	103	8	0.3
4	41:42	263	-9.77	1215	10	105	5	0.8
5	43	220	-5.81	1219	5	109	5	1.7
6	44	450	-3.17	1216	5	113	10	3.9
7	45	2401	-0.54	1228	10	145	8	22
8	46	1213	2.11	1245	5	128	5	9.5
9	47	300	4.75	1258	5	110	10	2.0
10	48:49	294	8.71	1252	13	108	5	0.8
11	50:52	233	15.31	1268	17	110	40	0.2
12	53:57	212	25.87	1257	17	69	5	0
13	58:68	~ 200	47.0	1302	6	36	20	0

angle of the slit must be close to the position angle of the major axis of this galaxy.

The spectrum has been searched very thoroughly for the presence of any Hβ or [O III] line emission. After the 4 h integration not a trace was found.

3.3. *Photometry*

The natural logarithm of the average countlevel as function of radius is shown in Fig. 16. On the bases of a disk with a scalelength of 25″ the bulge/disk ratio was determined and is given in Table 7. It is clear that the contribution of the bulge to the total light is considerable, centrally the bulge is completely dominant. Therefore one has to disentangle the bulge and disk in order to determine the influence of each of them on the kinematics.

For the disk density an exponential with constant thickness was assumed (van der Kruit and Searle, 1981):

$$\varrho(R,z) = \varrho_0 \, e^{-R/h} \, \mathrm{sech}^2\left(\frac{z}{z_0}\right), \tag{10}$$

where the photometric scalelength h was fixed to 25″ and the thickness parameter z_0 equal to 700 pc. For the *projected* bulge surface density an $R^{1/4}$ law was taken which is an excellent approximation for the majority of the bulges. The total bulge and disk projected surface density is given by

$$\Sigma(R) = \Sigma_e \exp\left\{-7.67\left[\left(\frac{R}{R_e}\right)^{1/4} - 1\right]\right\} + 2 z_0 \varrho_0^d \, e^{-R/h}, \tag{11}$$

where Σ_e is the surface density at one effective radius R_e and ϱ_0^d the central space density of the disk. A least squares fit of Eq. (11) was made to the slit intensities of Fig. 16 for both sides of the galaxy separately giving $\Sigma_e = 68$ and 408 counts, $R_e = 9''.23$ and $3''.22$ and $z_0 \varrho_0^d = 49$ and 59 arcsec × counts. There is quite some difference between the solution for both sides, but substituting the values into Eq. (11) the difference in surface density is only minor as can be seen in Fig. 16 where the solutions are plotted on top of the data.

In the next section a galaxy model will be employed to determine numerically the velocity dispersions. To this aim the 3-d density of the bulge is needed. This density distribution has to give the projected surface density as in Eq. (11). The deprojection of an $R^{1/4}$ law has been studied by Young (1976). I shall use essentially his formula for the bulge space luminosity density, with a slight alteration given by Van Albada (1988).

$$l = l_0 \exp\left(-b\left(\frac{R}{R_e}\right)^{1/4}\right)\left[\left(\frac{R}{R_e}\right)^{7/8} \cdot \left(1 + c\left(\frac{R}{R_e}\right)^{-7/8}\right)\right]^{-1}, \tag{12}$$

and

$$L_{tot} = \frac{4\pi R_e^3 \, l_0}{a}, \tag{13}$$

with $a = 656$, $b = 7.67$ and $c = 0.11$. The essential input parameter for the model calculations is l_0^b/l_0^d, the central light density of the bulge divided by that of the disk. For $R_e = 3''.22$ $l_0^b/l_0^d = 15600$ and for $R_e = 9''.23$ it is 1100. Integration of the total bulge light gives $L_{tot} = 0.93\ 10^5$ and $1.3\ 10^5$ for the two sides in count units and after calculation the total disk light on average $L_{tot}^{disk}/L_{tot}^{bulge} = 4.2$.

3.4. *The stellar velocity dispersion and M/L ratio*

The same kind of model analysis as in Sect. 2.6 has been performed for NGC 6340, only now the dispersion in the z-direction provides the major contribution to the observed values. The disk light distribution is as given by Eq. (10), and the bulge distribution as given by Eq. (12). Both the velocity dispersion in the radial and z-direction of the disk were assumed to be exponentially decreasing with a scalelength of 50″ ($=2h$) and $\langle v_z^2\rangle^{1/2}/\langle v_R^2\rangle^{1/2} = 0.6$. The bulge velocity dispersion was assumed to be constant. The model galaxy was given an inclination of 20° and the line profiles along the major axis were calculated, of which the dispersion can be compared with the observations. The result for a central disk z-dispersion $\langle v_z^2\rangle_{R=0}^{1/2}$ of 80, 100, and 120 km s^{-1} and bulge dispersion of 130 km s^{-1} is shown in Fig. 15. A few remarks should be made. First the dispersion curves as function of radius which are shown are an average for the two bulge/disk light distribution fits of the two sides. Fortunately the difference between the results for the two sides is at most ~5 km s^{-1}, the largest difference occurring near the radii where the bulge intensity equals the disk intensity. Because the galaxy has a 20° inclination also a tiny fraction of the velocity dispersion in the tangential direction enters into the integration. The net result is an increase of the calculated dispersion over the true z-dispersion of about 5% in the disk-dominated part. In fact the final line profiles are more or less a weighted addition of a broader bulge profile and a narrower disk profile. Even at radii around 5″ where the bulge is still dominant the disk dispersion is already noticeable.

Judging the fits to the data in Fig. 15 we may conclude that $\langle v_z^2\rangle_{disk,\,R=0}^{1/2} = 100 \pm 20$ km s^{-1} and that the bulge dispersion

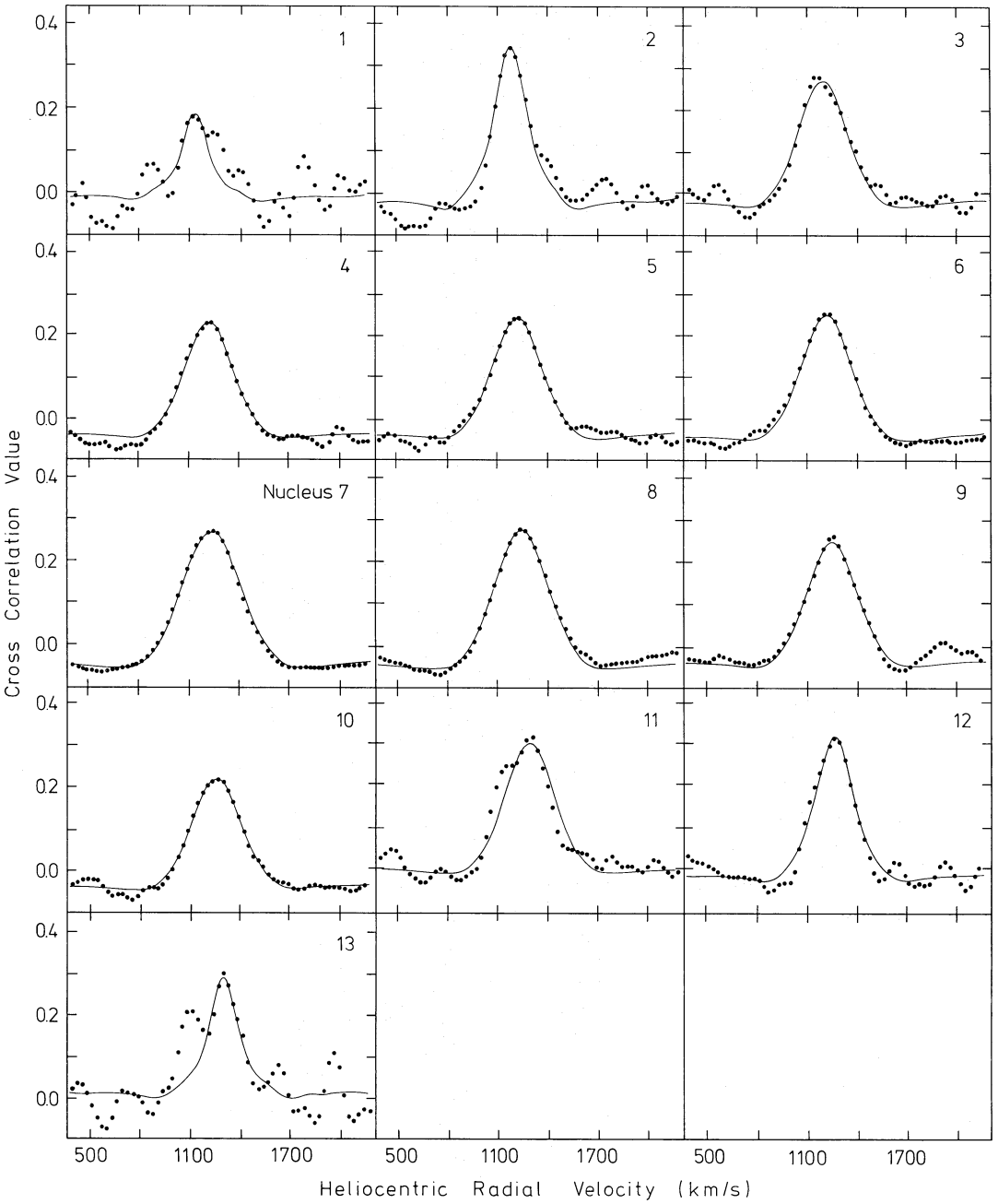

Fig. 13. The observed cross-correlation peaks for NGC 6340 (dots) with the best fitting model cross-correlation function (line) superposed. The numbers in the topright now correspond to the numbers in Table 7

$\langle v^2\rangle^{1/2}_{\rm bulge} = 130 \pm 10\,{\rm km\,s^{-1}}$. These fits are of course made under the assumption that the z-velocity dispersion is exponentially decreasing with a scalelength twice the photometric scalelength. A much longer observation would be needed to determine the exact radial behaviour of the disk velocity dispersion.

An estimate of the (constant) M/L ratio of the disk can be made because for an isothermal disk the velocity dispersion and mass are related by

$$\langle v_z^2\rangle^{1/2} = \sqrt{\pi G \sigma_0 z_0}\,, \tag{14}$$

implying that

$$\frac{M}{L} = 5.27 \left(\frac{\langle v_z^2\rangle^{1/2}_{R=0}}{50\,{\rm km\,s^{-1}}}\right)^2 \left(\frac{\sigma_0}{50\,L_\odot\,{\rm pc^{-2}}}\right)^{-1} \left(\frac{z_0}{0.7\,{\rm kpc}}\right)^{-1}, \tag{15}$$

where σ_0 is the projected central face-on surface density, and M/L is in solar units. The photometry by Wevers et al. (1986) in the J-band gives a central face-on surface density in the B band of 21.17 mag arcsec^{-2}. Conversion gives $\sigma_0 = 225\,L_\odot\,{\rm pc^{-2}}$ and $\langle v_z^2\rangle^{1/2}_{R=0} = 100 \pm 20\,{\rm km\,s^{-1}}$ with $z_0 = 700$ pc gives according to Eq. (15) $M/L = 4.7 \pm 1.5\,M_\odot/L_\odot$ in the B-band.

The mass-to-light ratio depends sensitively on the unknown scaleheight z_0. A value of 700 pc was used, which is an average value for the thickness of a number of Sb and Sc galaxies of "size"

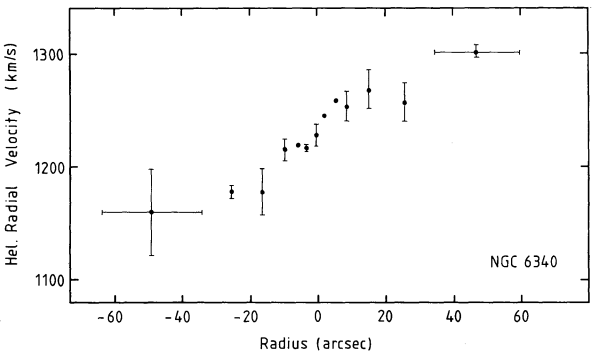

Fig. 14. Radial velocities along the slit for NGC 6340. A radius of zero is equal to the position of maximum intensity

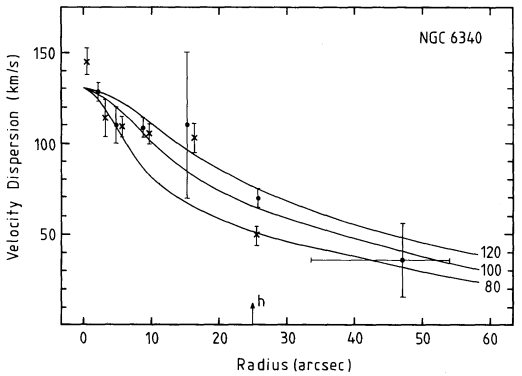

Fig. 15. The observed stellar velocity dispersions of NGC 6340 as a function of radius. The dots and crosses correspond to data for the different sides of the galaxy. The lines represent the results of the calculations of a bulge and disk model galaxy. The bulge dispersion was kept constant at 130 km s^{-1}, the disk z-velocity dispersion is decreasing exponentially (scalelength = 2h) with central values of 80, 100, and 120 km s^{-1}

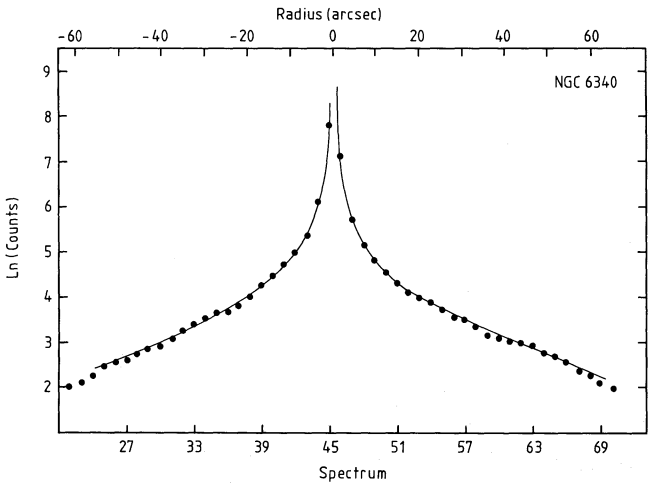

Fig. 16. The logarithm of the average number of counts over the 1000 Å wavelength range as function of radius. The curves are the results of a least squares fit to the data for a combined $R^{1/4}$ bulge and exponential disk

$V_{max} = 200$ km s^{-1} as found by van der Kruit and Searle (1982). Whether this extrapolation from early types to Sa is valid remains very uncertain. Therefore onle tentatively a comparison can be made between the M/L ratios of NGC 6340 and of the face-on Sc galaxy NGC 5247 (van der Kruit and Freeman, 1986). Both galaxies are of comparable size and the M/L ratios were calculated from the observed velocity dispersions assuming $z_0 = 700$ pc. For NGC 5247 $M/L = 5 \pm 2\, M_\odot/L_\odot$ for the old disk population alone. The M/L ratio of 4.7 ± 1.5 for NGC 6340 is also for the old disk population because the $B-V$ colour for this galaxy is constant with radius, around 0.92, which is rather red signifying that there is hardly any light originating from a young population.

Recent infrared photometry of edge-on galaxies (Wainscoat, 1986) possibly suggests that at small heights above the disk a deviation from isothermal conditions occurs. This implies that for the calculation of the M/L values from the observed photometry and velocity dispersion equation 15 cannot be used any more. It turns out that (see van der Kruit, 1988) the M/L ratio has to be increased by $\sim 25\%$ compared to the "isothermal" value. This increase, of course, would apply for all face-on galaxies.

4. Conclusions

On the bases of the observations of NGC 6503 and subsequent modelling it can be concluded that the stellar velocity dispersion in the radial direction is decreasing exponentially with radius with a scalelength twice the photometric scalelength. At $R = h$ the dispersion amounts to 33 ± 6 km s^{-1}. This radial behaviour produces an almost constant Q with radius, or, if a model with constant Q is employed it fits the data also quite satisfactory. A sharp drop in the observed velocity dispersion for $R < 11''$, however, cannot readily be explained. Probably the lack of scatterers like spiral arms and the small rotation near the central region prevents the stars to heat up at these radii. In B88 a velocity dispersion versus luminosity and velocity dispersion versus max. rotational velocity relation was given for a few galactic disks. The values for NGC 6503 also fit very nicely into this relation. A constant Q value of 1.7 gives a total mass-to-light ratio in the B-band of 1.7 ± 0.3 (for the old disk only: $(M/L)_B = 2.1 \pm 0.3$) which is in perfect agreement with the M/L value of 1.7 inferred from a fit of the photometry to the rotation curve and assuming the maximum disk hypothesis.

For the face-on galaxy NGC 6340 a bulge-disk light decomposition has been made. For modelling the observed spectroscopic results this is necessary because the bulge light contribution is quite substantial. Under the assumption of constant M/L and disk thickness and consequent exponential decreasing velocity dispersion it turned out that centrally $\langle v_z^2 \rangle^{1/2}_{R=0} = 100 \pm 20$ km s^{-1} and that the bulge dispersion is around 130 km s^{-1}. A M/L ratio of 4.7 ± 1.5 in the B-band was found which is about equal to the $M/L = 5 \pm 2$ for the face-on Sc galaxy NGC 5247.

Acknowledgements. The author wishes to thank R. le Poole and V. Reyes for their assistance at the telescope during the observations. I also thank A. Pickles for introducing me to the software package Pandora, the staff of the Netherlands Foundation for Radio Astronomy for letting me use their computer facilities in order to reduce the data, R. Peletier for taking two CCD frames of NGC 6503 and P. van der Kruit for valuable advise and encouragement during the course of this project. Finally I thank T.S. van Albada for a close scrutiny of the original manuscript and for giving many suggestions for improvement.

References

Albada, T.S. van: 1988 (private communication)
Athanassoula, E., Sellwood, J.A.: 1986, *Monthly Notices Roy. Astron. Soc.* **221**, 213
Begeman, K.: 1987, Ph. D. Thesis, Groningen State University
Bertola, F., Bernacca, P.L.: 1967, *Memorie Soc. Astron. Ital.* **38**, 189
Binney, J., Lacey, C.: 1988, *Monthly Notices Roy. Astron. Soc.* **230**, 597
Bottema, R.: 1988, *Astron. Astrophys.* **197**, 105
Bottema, R., Kruit, P.C., van der, Freeman, K.C.: 1987, *Astron. Astrophys.* **178**, 77
Carlberg, R.G., Sellwood, J.A.: 1985, *Astrophys. J.* **292**, 79
Efstathiou, G., Lake, G., Negroponte, J.: 1982, *Monthly Notices Roy. Astron. Soc.* **199**, 1069
Freeman, K.C.: 1970, *Astrophys. J.* **160**, 811
Gunn, J.E., Stryker, L.L.: 1983, *Astrophys. J. Suppl.* **52**, 121
Kruit, P.C. van der: 1988, *Astron. Astrophys.* **192**, 117
Kruit, P.C. van der, Freeman, K.C.: 1984, *Astrophys. J.* **278**, 81
Kruit, P.C. van der, Freeman, K.C.: 1986, *Astrophys. J.* **303**, 556
Kruit, P.C. van der, Searle, L.: 1981, *Astron. Astrophys.* **95**, 105
Kruit, P.C. van der, Searle, L.: 1982, *Astron. Astrophys.* **110**, 61
Lewis, J.R.: 1987, Ph. D. Thesis, Australian National University
Longo, G., de Vaucouleurs, A.: 1983, *A General Catalogue of Photoelectric Magnitudes and Colors in the U, B, V system of 3578 Galaxies Brighter than the 16th Magnitude*, University of Texas Monographs in Astronomy, No. 3
Moorsel, G.A. van, Wells, D.C.: 1985, *Astron. J.* **90**, 1038
Ostriker, J.P., Peebles, P.J.E.: 1973, *Astrophys. J.* **186**, 467
Sandage, A., Tammann, G.A.: 1981, *A Revised Shapley-Ames Catalog of Bright Galaxies*, Carnegie Institute of Washington
Sellwood, J.A., Carlberg, R.G.: 1984, *Astrophys. J.* **282**, 61
Spitzer, L., Schwarzschild, M.: 1951, *Astrophys. J.* **114**, 385
Toomre, A.: 1964, *Astrophys. J.* **139**, 1217
Vaucouleurs, G. de, Caulet, A.: 1982, *Astrophys. J. Suppl.* **49**, 515
Villumsen, J.V.: 1985, *Astrophys. J.* **290**, 75
Wainscoat, R.J.: 1986, Ph. D. Thesis, Australian National University
Wevers, B.M.H.R.: 1984, Ph. D. Thesis, Groningen State University
Wevers, B.M.H.R., Kruit, P.C. van der, Allen, R.J.: 1986, *Astron. Astrophys. Suppl.* **66**, 505
Young, P.J.: 1976, *Astron. J.* **81**, 807